Supplementary Information

Supplementary Figure 1.

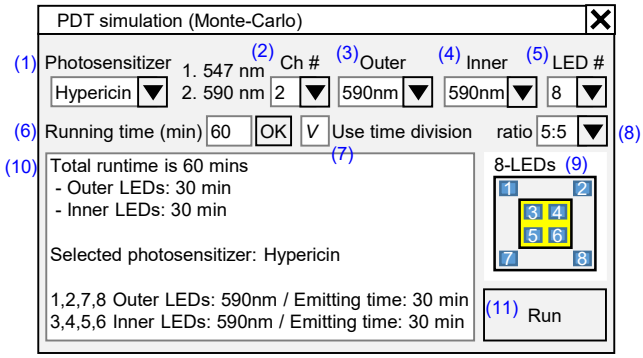

	Setup value	Description
1	Photosensitizer type	Select the photosensitizer type; this version supports Foscan or Hypericin information.
2	The number of channels	Select how many channels use in the simulation.
3	Outer LED spectrum	Choose the spectrum of the outer LED, the location depends on the (5), the total number of LEDs
4	Inner LED spectrum	Choose the spectrum of the inner LED, the location depends on the (5), the total number of LEDs
5	The total number of LEDs	Select the total number of LEDs in a device.
6	Total runtime	Input the total running time of the simulation.
7	Time division function usage	Check whether to use the time division function or not.
8	The ratio of usage of outer and inner LED	If the user checked on (7), select the ratio of time division of LED usages.
9	Show the design of LEDs	Depends on the (5), it shows the design of the device
10	Description of setup values	All setup values are shown here.
11	Start button	If the setting values are okay, run the simulation. If not, it shows an error message.

Supplementary Figure 1. A representative image of a user interface software and detailed descriptions of parameter settings.

Supplementary Figure 2.

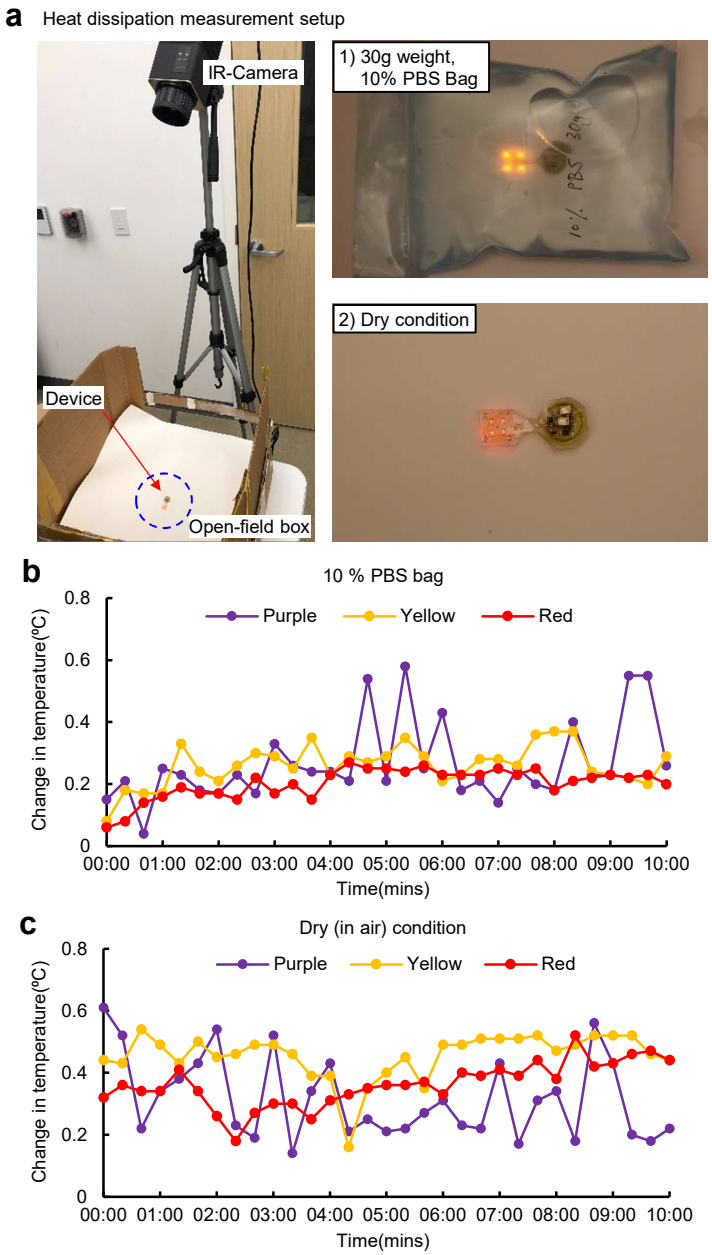

Supplementary Figure 2. (**a**) Pictures of an experimental setup for wireless measurements of heat dissipation using IR camera (left). Here, TX power is set to 4 W. The two right images show a device mounted on sealed bag of 10 % PBS saline solution (right to the top), and itself in a cage (right to the bottom), respectively. Plots of optical intensity as a function of time at duty cycles - 25 % with 10-ms pulse train - in each condition; 10 % PBS bag (**b**), and dry (**c**).

Supplementary Figure 3.

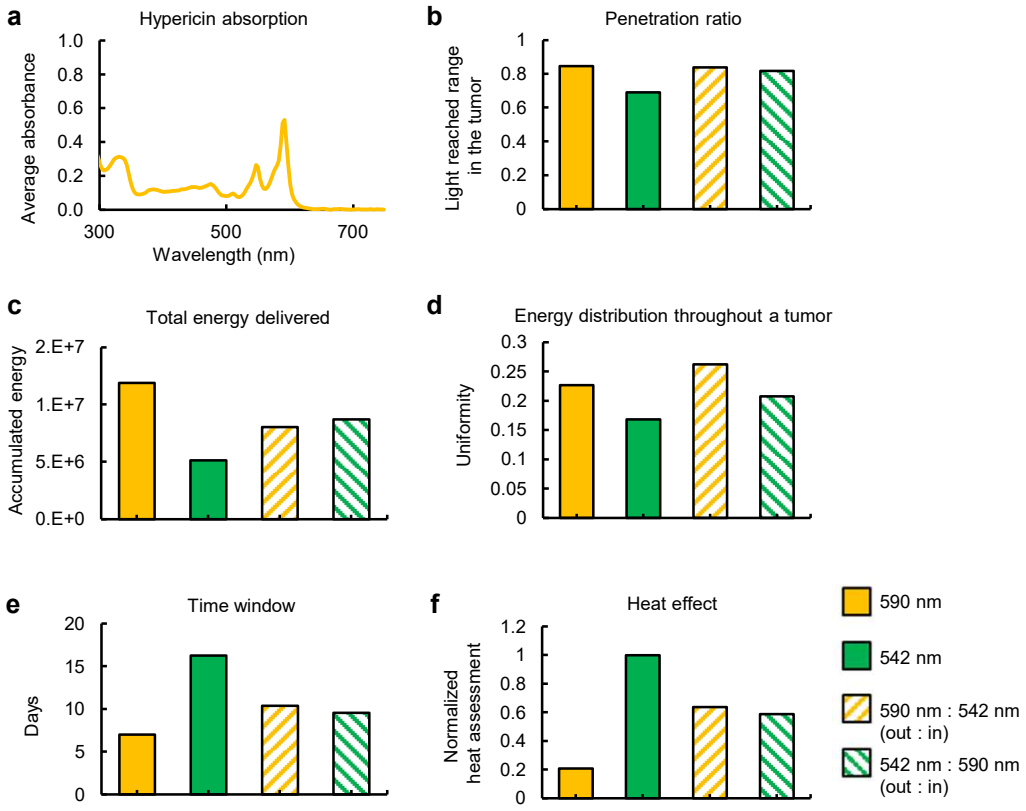

Supplementary Figure 3. Summary of simulation results for Hypericin treatment. (**a**) Averaged light absorbance spectrum of Hypericin: Peaks are located at 590 nm and 542 nm, respectively. (**b**) The percentage of the light energy bins reached in a tumor at various wavelengths. (**c**) Total energy delivered to a tumor at various wavelengths. (**d**) Energy distribution through a tumor at various wavelengths. (**e**) Time window during which experiments occur. Here, a total energy of 12 J cm^{-3} is required for hindering tumor growth. Duty-cycle of light sources and light intensity determine the time window. (**f**) Normalized heat variation at various wavelength conditions. Results suggest that the use of light sources with a wavelength of 590 nm leads to minimum heat dissipation and maximum light absorption.

Supplementary Figure 4.

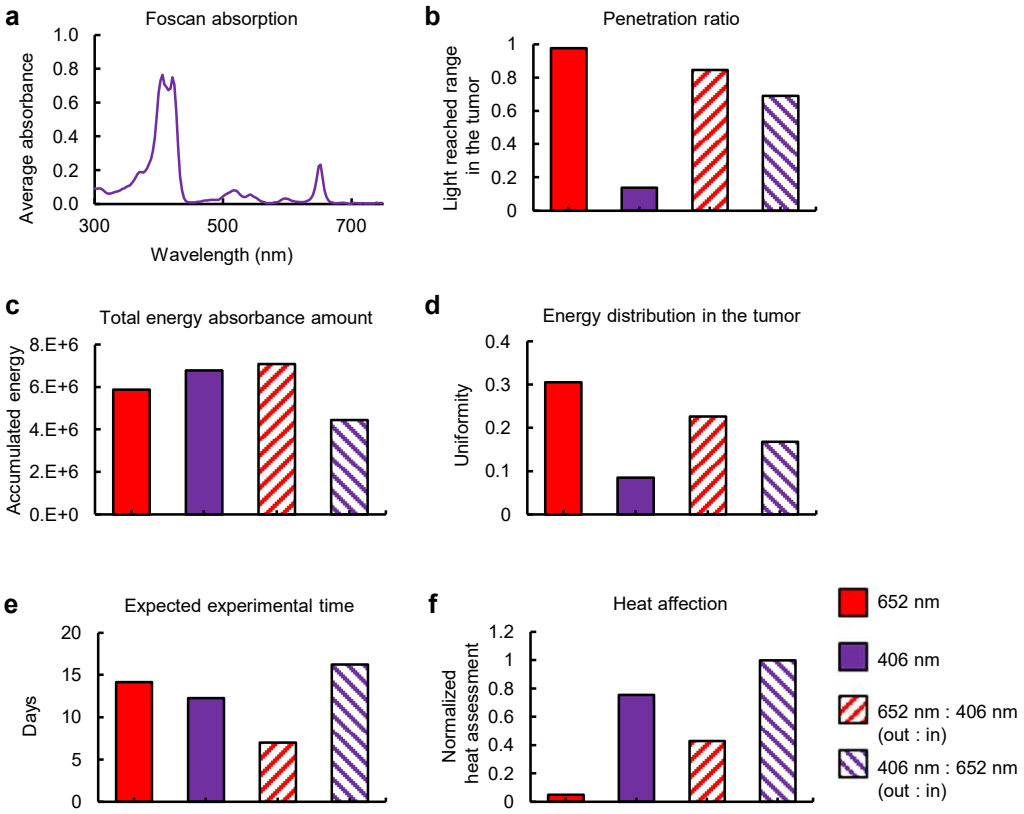

Supplementary Figure 4. Summary of simulation results for Foscan treatment. (**a**) Averaged light absorbance spectrum of Foscan: Peaks are located at 406 nm and 652 nm, respectively. (**b**) The percentage of the light energy bins reached in a tumor at various wavelengths. (**c**) Total energy delivered to a tumor at various wavelengths. (**d**) Energy distribution through a tumor at various wavelengths. (**e**) Time window during which experiments occur. Here, a total energy of 12 J cm^{-3} is required for hindering tumor growth. Duty-cycle of light sources and light intensity determine the time window. (**f**) Normalized heat variation at various wavelength conditions. Results suggest that the use of light sources with a combination of wavelengths of 652 nm (out) and 406 nm (in) leads to minimum heat dissipation and maximum light absorption.

Supplementary Figure 5.

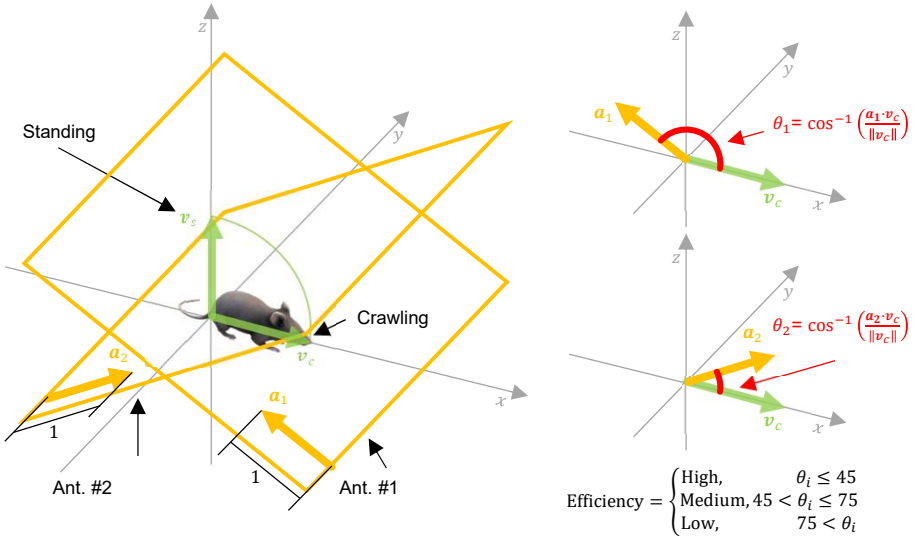

Supplementary Figure 5. Illustrative representations of $\boldsymbol{v}$ (an implantable device) and $\boldsymbol{a}_1$ & $\boldsymbol{a}_2$ (Ant. # 1 & 2). The relative angle θ_i between $\boldsymbol{v}$ and $\boldsymbol{a}_i$ determines the power transmission efficiency.

Supplementary Figure 6.

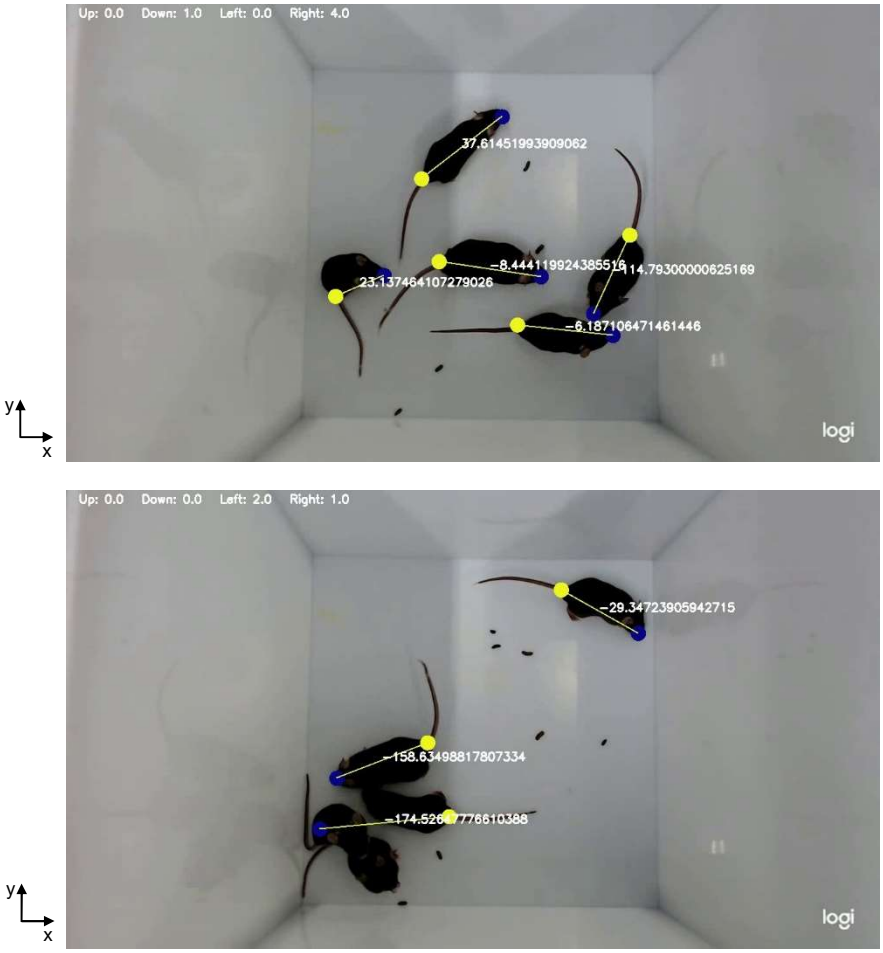

Supplementary Figure 6. Two representative images processed by the AI algorithm. The top image shows perfect alignments of five vectors with a selected coil antenna while the bottom image includes only three vector assignments. It is likely for the two non-assigned mice (or implanted devices) to receive not enough power due to a misalignment between an implanted device and a selected coil antenna. However, a supercapacitor embedded in an implantable device can store power while harvesting energy from the TX system. Thus, it can still illuminate light sources when power delivery is not enough. Measurement results in supplementary Fig. 8 support this expectation.

Supplementary Figure 7.

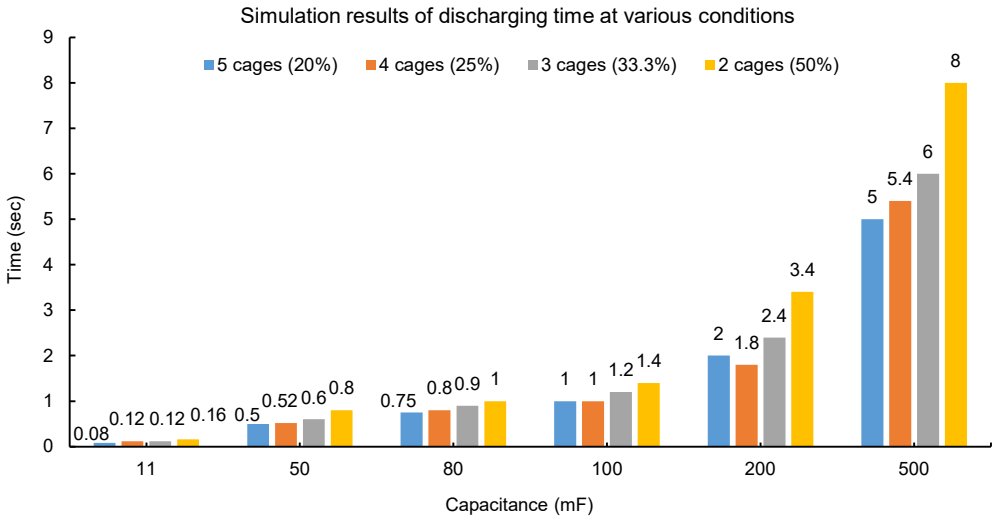

Supplementary Figure 7. Simulation results of discharging time at various conditions; different capacity and number of cages. Results suggest that a supercapacitor with a capacity of 11-mF can maintain light intensity enough for activation of a photosensitizer when not in powered by the TX system (during off-cycle).

Supplementary Figure 8.

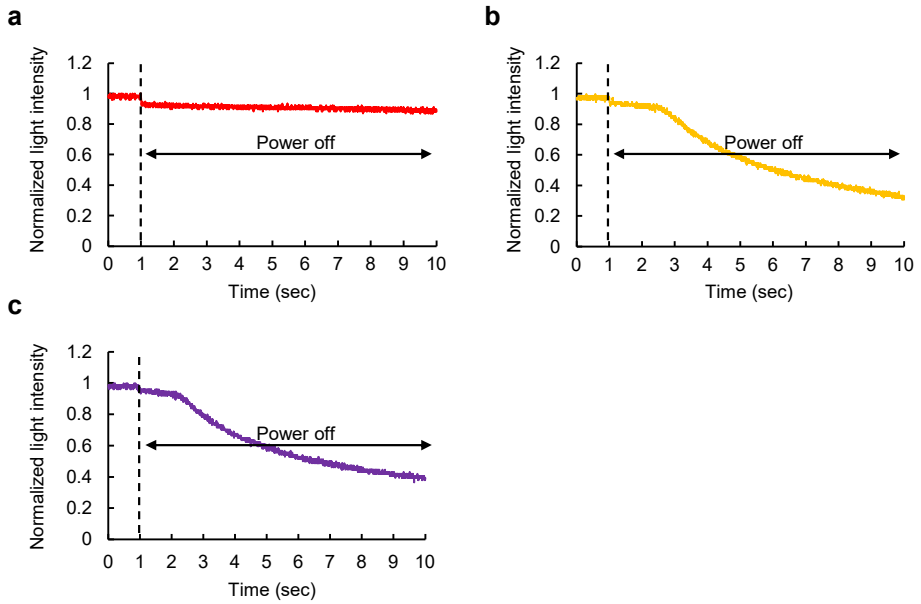

Supplementary Figure 8. Measurement results of light intensity during discharging. (**a**) red: 652 nm, (**b**) yellow: 590 nm, and (**c**) purple: 406 nm, respectively.

Supplementary Figure 9.

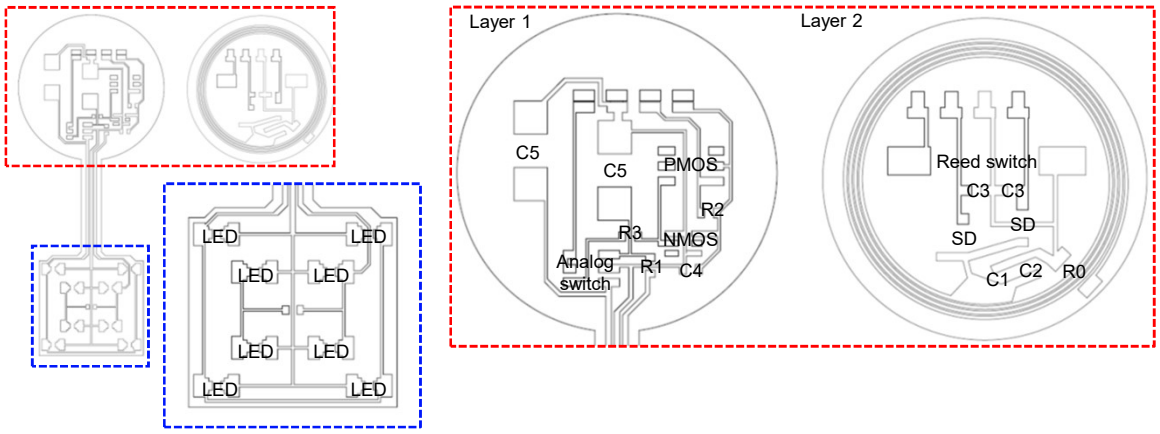

	Components	Product number	Vendor information
LED1	405nm, 1.6 mm x 0.8 mm x 0.8 mm	A-0603UUVC	Lighthouse LEDs
LED2	591nm, 0.65 mm x 0.35 mm x 0.2 mm	APG0603SYC-TT	Kingbright
LED3	632nm, 0.65 mm x 0.35 mm x 0.2 mm	APG0603SEC-E-TT	Kingbright
SD	Schottky Diode, 1.4 mm x 0.6 mm x 0.52 mm	DB27309	Panasonic
R0	0 ohm, 1.6 mm x 0.9 mm x 0.55 mm	RCWPM-0603	VISHAY
R1	0 ohm, 1.00 mm x 0.55 mm x 0.35 mm	RCWPM-0402	VISHAY
R2	20 kohm, 0.6 mm x 0.3 mm x 0.23 mm	RC0603F203CS	Samsung Electro-Mechanics
R3	4.99 kohm, 0.6 mm x 0.3 mm x 0.23 mm	RC0603F4991CS	Samsung Electro-Mechanics
C1	100 pF, 0.6 mm x 0.3 mm x 0.33 mm	CL03C820JA3NNNC	Samsung Electro-Mechanics
C2	330 pF, 0.6 mm x 0.3 mm x 0.33 mm	CL03B331KA3NNNC	Samsung Electro-Mechanics
C3	1 μF, 0.6 mm x 0.3 mm x 0.33 mm	CL03A105KP3NSNC	Samsung Electro-Mechanics
C4	0.1 μF, 0.6 mm x 0.3 mm x 0.33 mm	CL03A104KP3NNNC	Samsung Electro-Mechanics
C5	11 mF, 3.2 mm x 2.5 mm x 0.9 mm	CPH3225A	Seiko Instruments
NMOS	1.0 mm x 1.0 mm x 0.34 mm	NTUD3170NZ	ON Semiconductor
PMOS	1.7 mm x 1.7 mm x 0.6 mm	NX3008PBKV	Nexperia
Reed Switch	7.0 mm x 2.2 mm x 1.6 mm	MK24-A-2	Standex Meder electronics
Analog Switch	1.6 mm x 1.2 mm x 0.6 mm	SN74LVC1G3157	Texas Instruments

Supplementary Figure 9. Device layout (top) and a table of components used for an implantable wireless device (bottom).

Supplementary Figure 10.

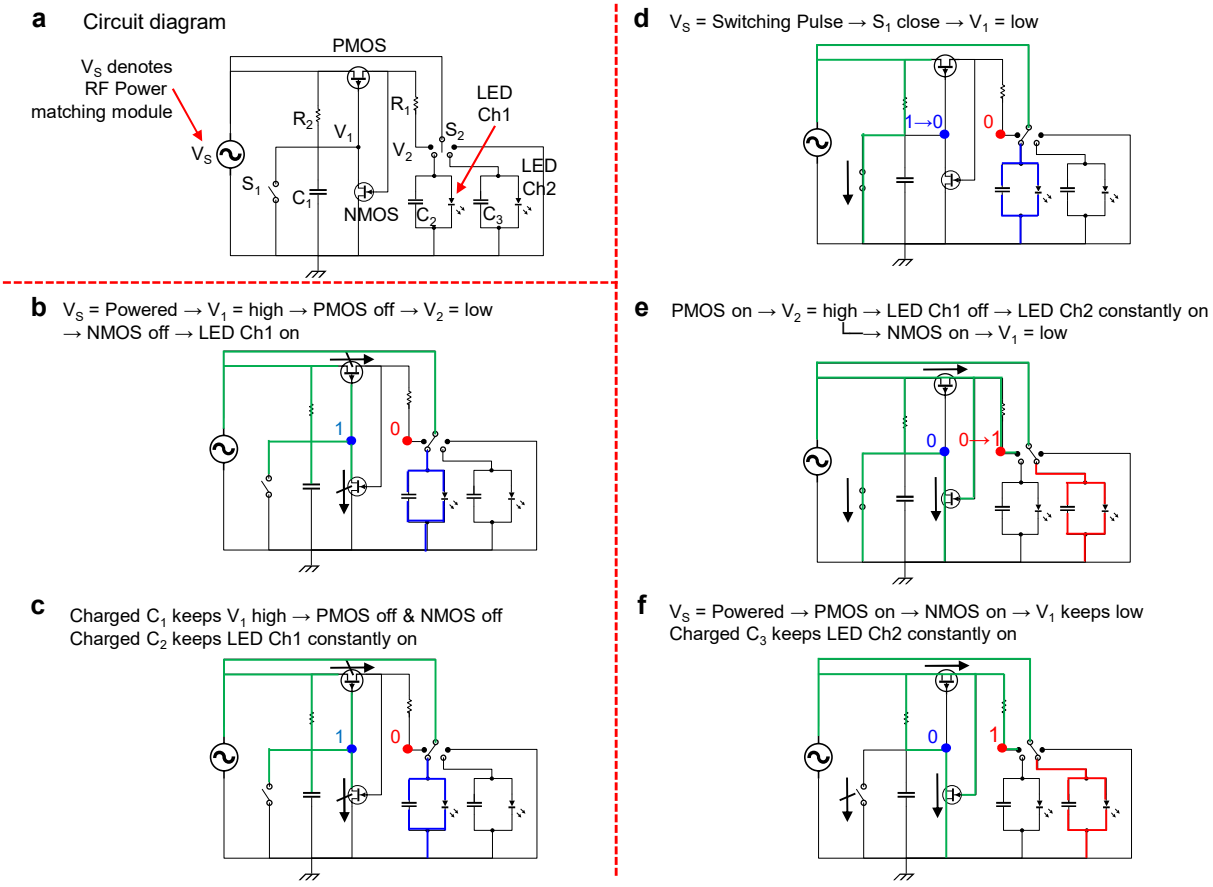

Supplementary Figure 10. (**a**) Circuit diagrams of an implantable device for multi-wavelength operation. Here, a dual-channel device automatically activates a channel in response to signals from a remotely located wireless TX system. R_1 = 5kΩ, R_2 = 20kΩ, C_1 = 100pF, C_2 = C_3 = 11mF, a reed switch is denoted by S_1, and S_2 denotes an analog switch. (**b**), (**c**) Signal-flows from a power supply to Ch1 LED for Ch1 activation. (**d**)-(**f**) Signal-flows during switching from Ch1 to Ch2.

Supplementary Figure 11.

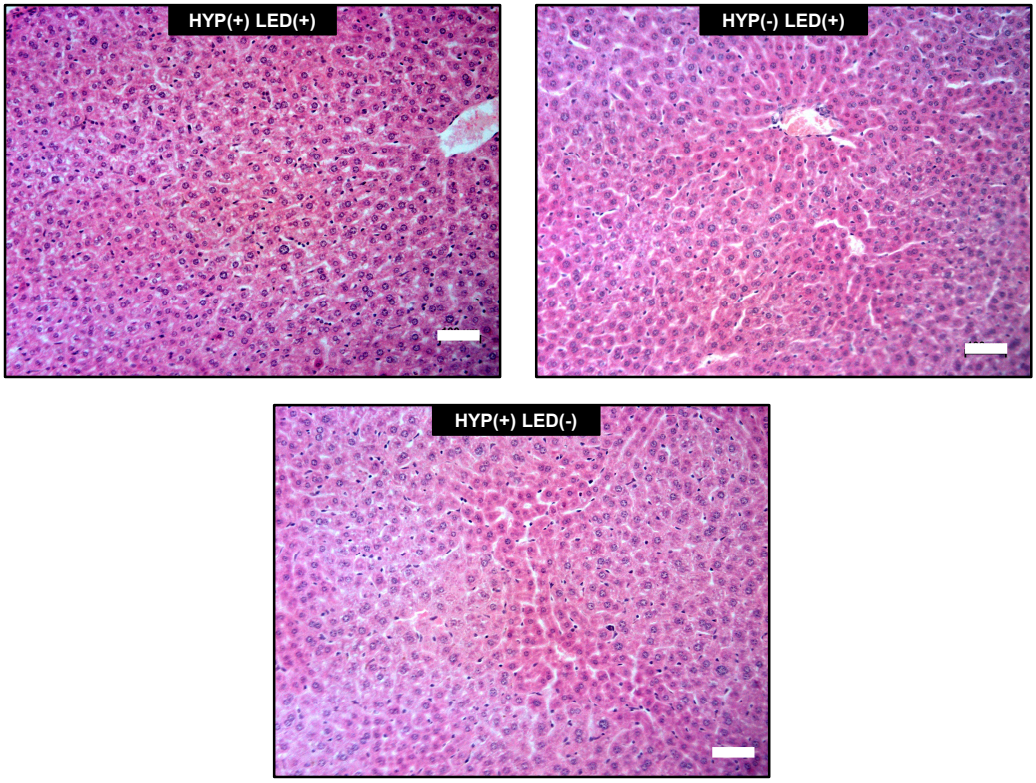

Supplementary Figure 11. Images of H&E stained sections of livers from mice in the different treatment groups: scale bar 100 μm.

Supplementary Figure 12.

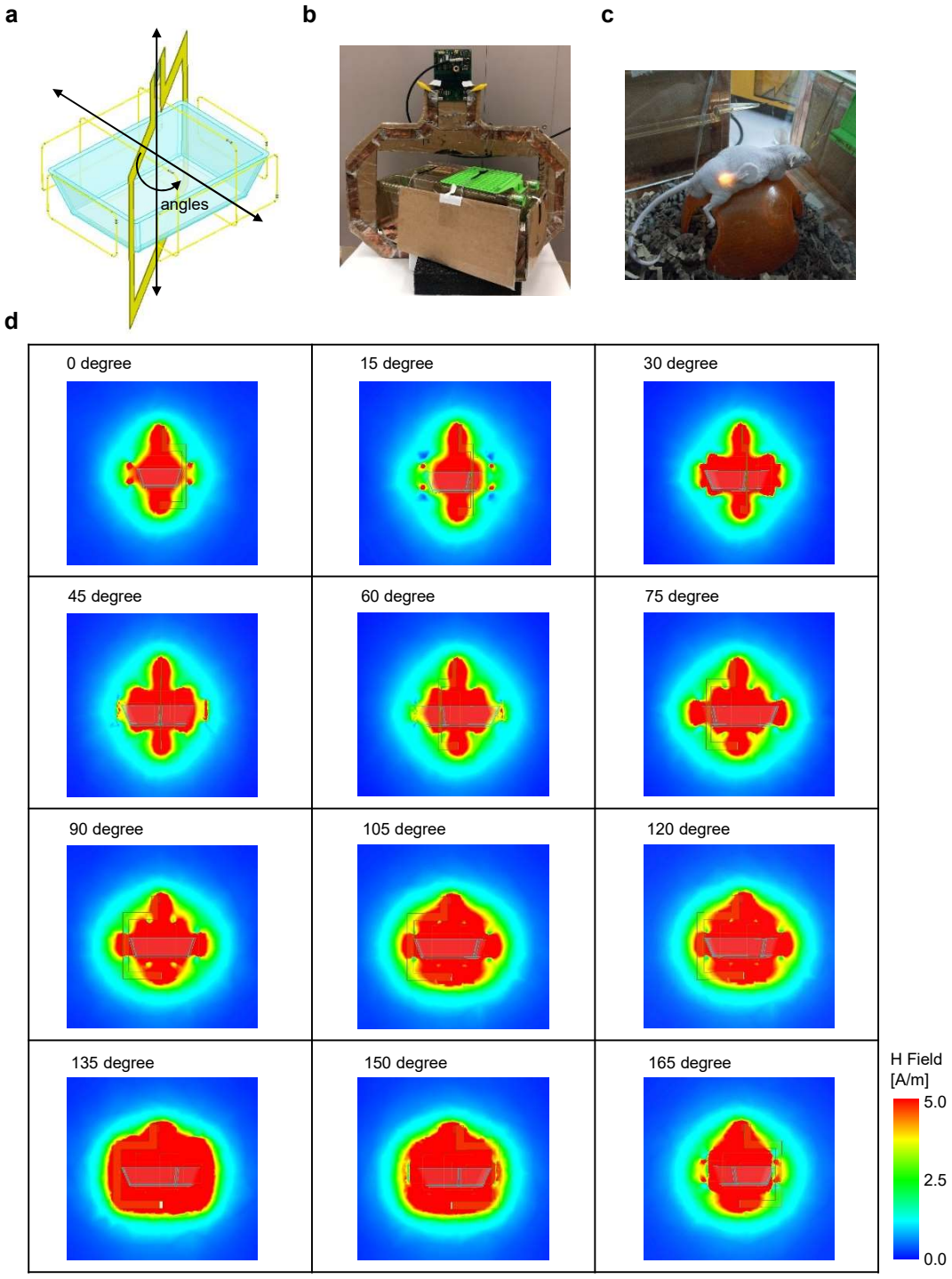

Supplementary Figure 12. (**a**) Illustration of the vertical structured antennas for flank implantation in a mouse. (**b**) A photo of the antenna setup and cage. (**c**) A photo of an animal with a device implanted. (**d**) Simulation results of a vertical structured antenna at various angles. Results reveal that the proposed structure offers uniform wireless coverage enough for activation of a photosensitizer throughout the volume of a cage.

Supplementary Figure 13.

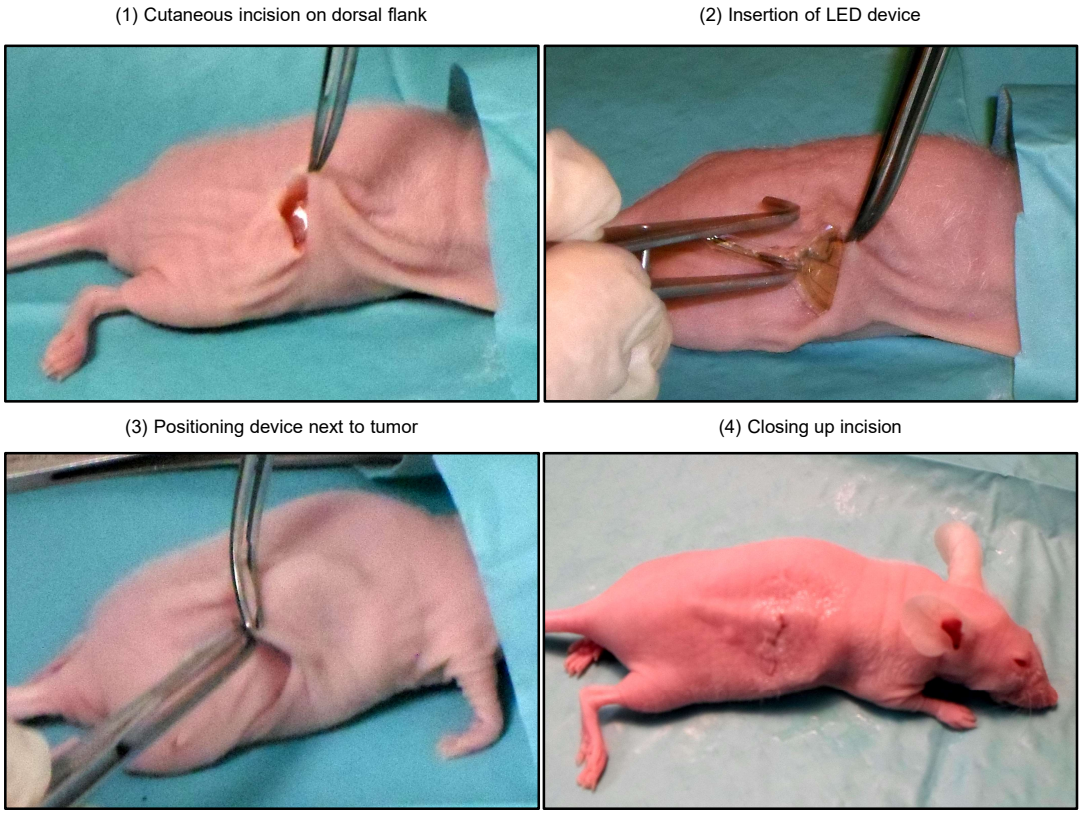

Supplementary Figure 13. Step-by-step procedures for device implantation.